



Universiteit
Leiden

The Netherlands

Inflammation in injury-induced vascular remodelling : functional involvement and therapeutical options

Schepers, A.

Citation

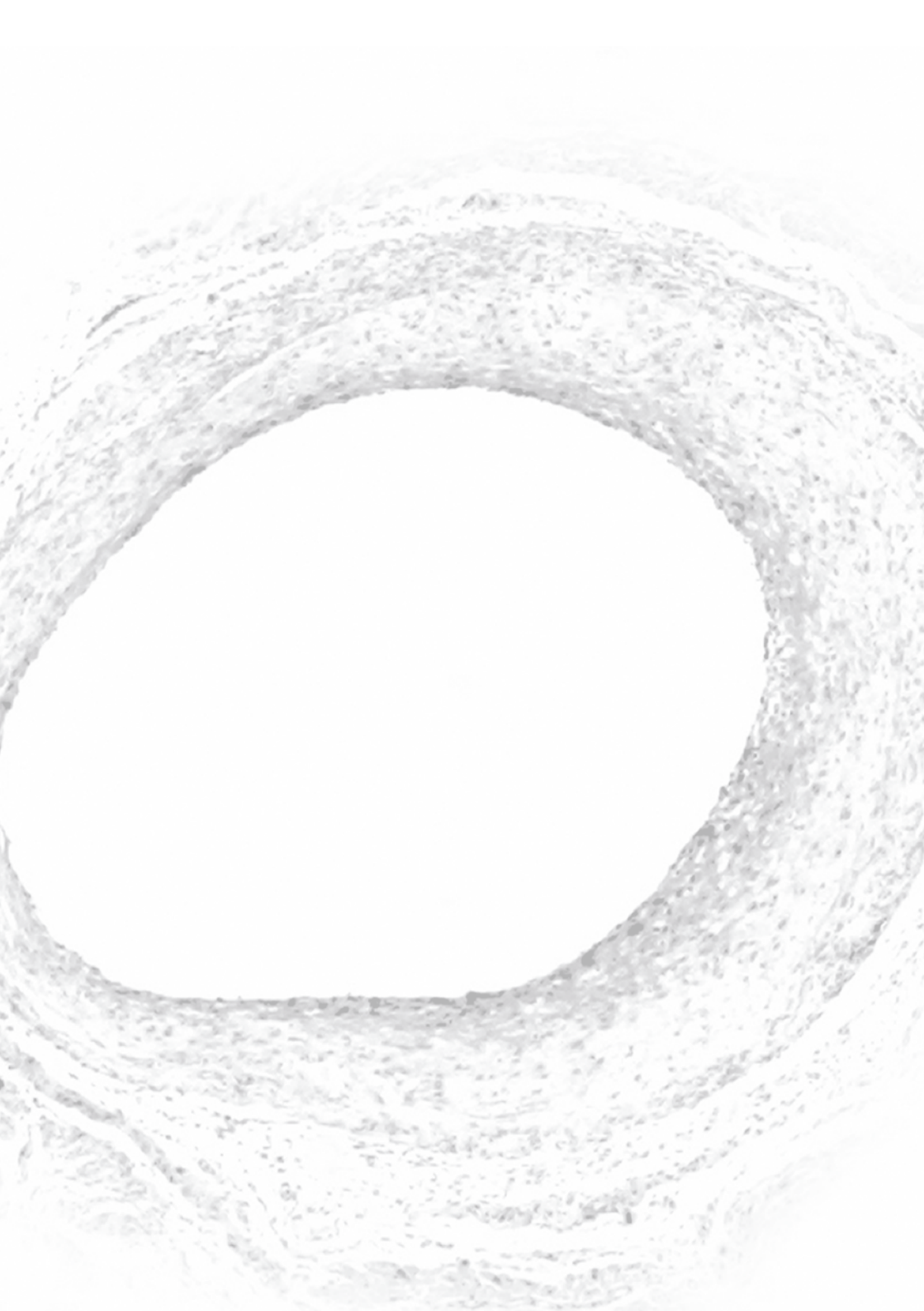
Schepers, A. (2008, April 9). *Inflammation in injury-induced vascular remodelling : functional involvement and therapeutical options*. TNO Quality of Life, Gaubius Laboratory, Faculty of Medicine / Leiden University Medical Center (LUMC), Leiden University. Retrieved from <https://hdl.handle.net/1887/12687>

Version: Corrected Publisher's Version

License: [Licence agreement concerning inclusion of doctoral thesis in the Institutional Repository of the University of Leiden](#)

Downloaded from: <https://hdl.handle.net/1887/12687>

Note: To cite this publication please use the final published version (if applicable).



APPENDICIES

Colour Figure Overview

LEGENDS CHAPTER 1

Figure 1.1: Schematic representation (A) and microphotograph (B) of femoral artery cuff positioning.

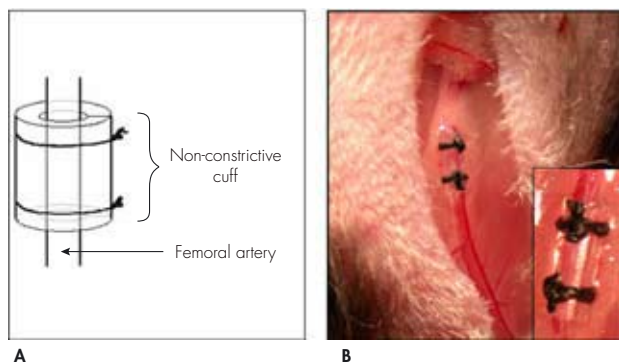
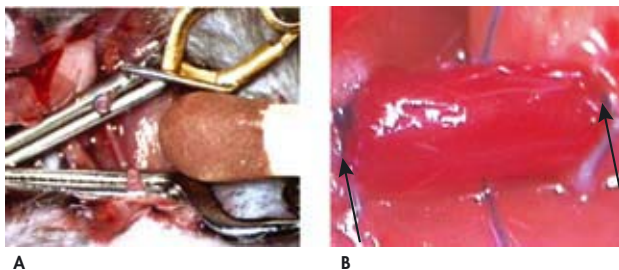


Figure 1.2: Bypass model in a mouse. Panel A: The common carotid artery is divided and occluded with 2 clamps. The inferior caval vein of a donor mouse will be implanted as interposition. Panel B: Venous interponate in situ, arrows indicate anastomotic side.



LEGENDS CHAPTER 2

Figure 2.1: Representative cross-sections of cuffed murine femoral arteries. A: Placebo treatment. **B:** *i.p.* dexamethasone treatment. **C:** Oral dexamethasone treatment. HPS staining, magnification 400x (arrow indicates the internal elastic lamina; arrowheads indicate the external elastic lamina). **D:** Total intimal area of cuffed murine femoral arteries 21 days after cuff placement. Total intimal area was quantified by image analysis using ten serial cross-sections from each cuffed artery and expressed in μm^2 (mean \pm SEM, $n=6$). NS, $P>0.05$ (NS, not significant); ** $P<0.01$.

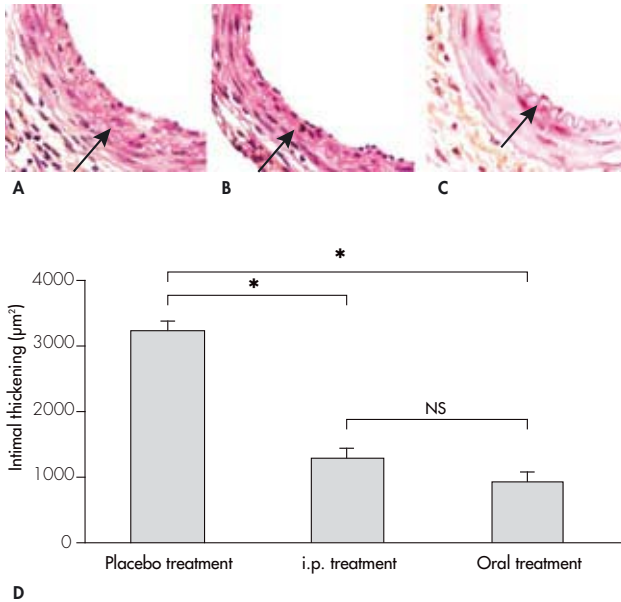


Figure 2.3: Representative cross-sections of cuffed murine femoral arteries treated with increasing concentrations of dexamethasone 21 days after cuff placement. A: Control empty drug-eluting PCL cuff. B: 1% (w/w) dexamethasone-eluting PCL cuff. C: 5% (w/w) dexamethasone-eluting PCL cuff. D: 20% (w/w) dexamethasone-eluting PCL cuff. HPS staining, magnification 400x (arrow indicates the internal elastic lamina; arrowheads indicate the external elastic lamina). E: Total intimal area of cuffed murine femoral arteries 21 days after drug-eluting PCL cuff placement. Total intimal area was quantified by image analysis using ten serial cross-sections from each cuffed artery and expressed in μm^2 (mean \pm SEM, n=6). NS, $P>0.05$ (NS, not significant); * $P<0.05$; ** $P<0.01$.

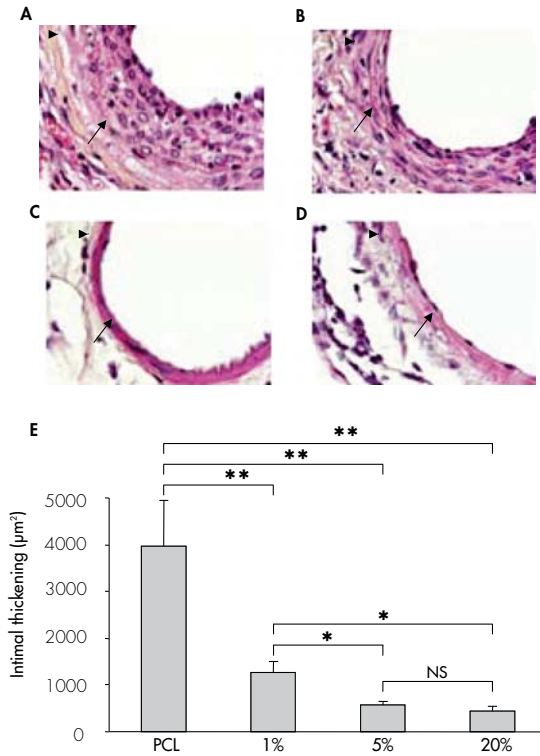


Figure 2.4: Histomorphometrical quantification of cuffed femoral arteries treated with increasing concentrations of dexamethasone. Percentage of TUNEL-positive nuclei (A), total medial area (B) and internal elastic lamina (IEL) disruption (C) of cuffed femoral arteries treated with increasing concentrations of dexamethasone 21 days after drug-eluting PCL cuff placement. TUNEL-positive nuclei were counted in six equally spaced cross-sections from each cuffed artery and expressed as a percentage of the total number of nuclei. Medial area was quantified by image analysis using ten serial cross-sections in each cuffed artery and expressed in μm^2 . IEL disruption was assessed in ten serial cross-sections from each cuffed femoral artery and expressed as the number of broken IEL per cuffed artery segment. Mean \pm SEM, n=6. NS, P>0.05 (NS, not significant); *P<0.05.

Inserts: A: TUNEL staining; femoral artery segments locally treated with 20% (w/w) dexamethasone (20% Dexa) show an increase in TUNEL-positive nuclei as compared to control empty PCL (PCL) cuffed segments. Arrows indicate TUNEL-positive nuclei, magnification 600x. **B:** Weigert's elastin staining; cuffed artery segments treated with 20% (w/w) dexamethasone show a striking medial atrophy. Bars indicate cross-sectional medial area, magnification 600x. **C:** Weigert's elastin staining; control empty PCL cuffed femoral arteries show an intact IEL while local delivery of dexamethasone enhances IEL disruption. Arrows indicate IEL disruption, magnification 600x.

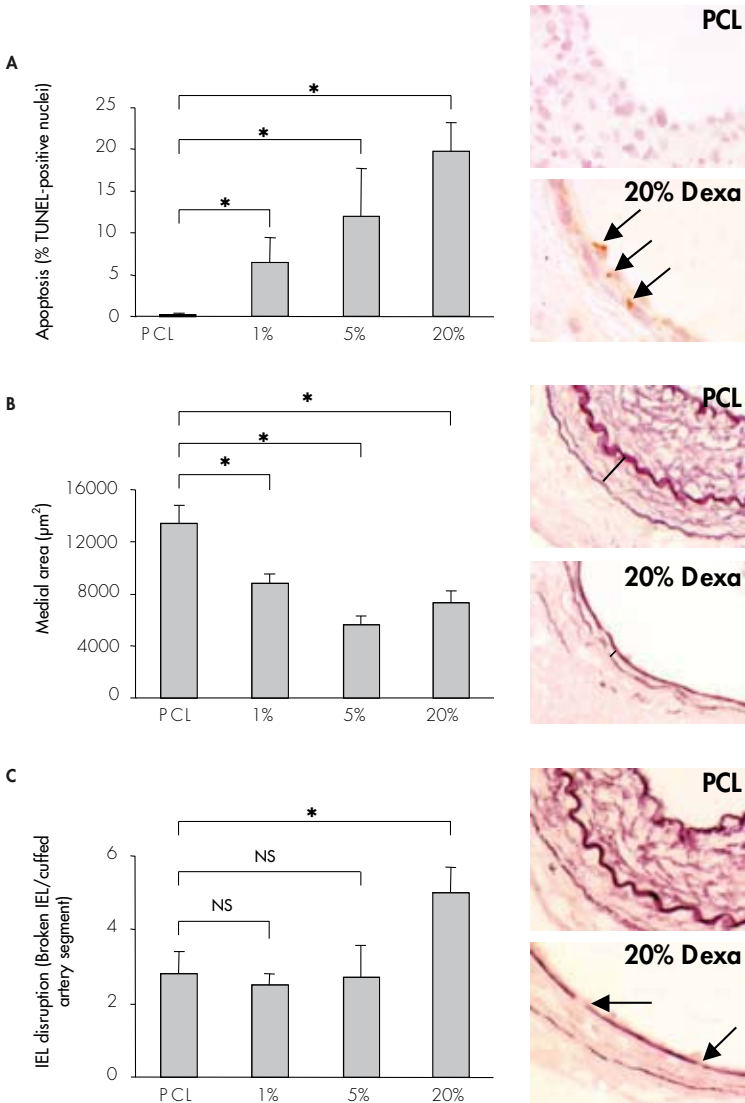
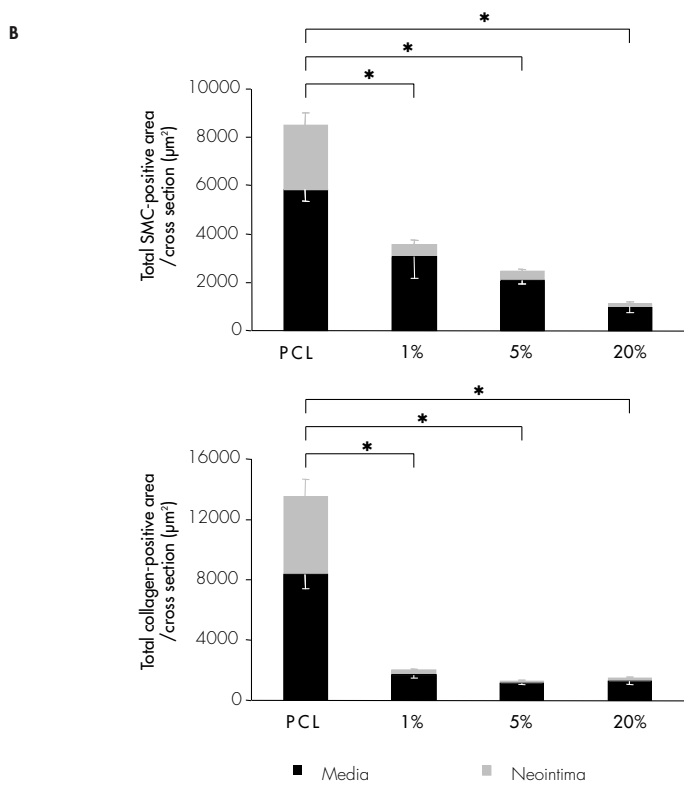
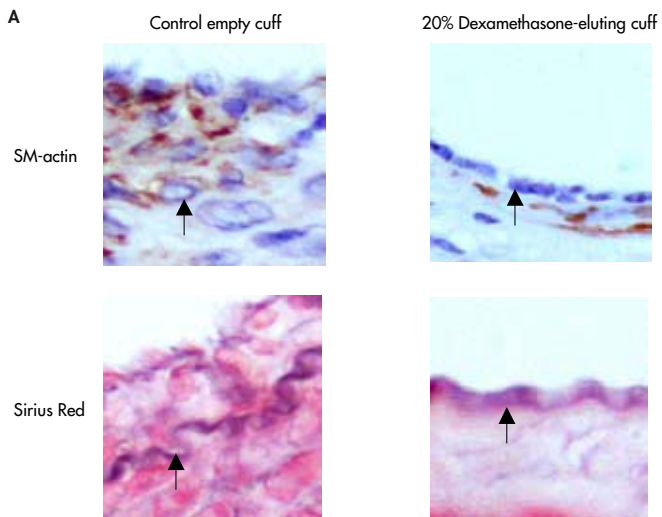


Figure 2.5: A: Representative cross-sections of cuffed murine femoral artery 21 days after placement of either a control empty PCL cuff or a 20% (w/w) dexamethasone-eluting PCL cuff. Alpha smooth muscle cell actin staining for smooth muscle cells; a striking decrease in alpha SMC-positive cells content is observed in the cuffed vessel perivascularly treated with dexamethasone. Sirius red stain for collagen; a reduced vascular collagen content is present in vessel segments locally treated with dexamethasone. Magnification 600x (arrow indicates the internal elastic lamina). **B:** Total SMC- (top) and collagen-positive (bottom) area of cuffed murine femoral arteries treated with increasing concentrations of dexamethasone at 21 days after drug-eluting PCL cuff placement. SMC- and collagen-positive areas were quantified both in the media (black bars) and in the neointima (grey bars) by image analysis using six serial sections in each cuffed artery and expressed in μm^2 . Mean \pm SEM, n=6. *P<0.05.



LEGENDS CHAPTER 3

Figure 3.1: Effect of IL10 knock-out on neointimal formation in hypercholesterolemic mice. Total intimal thickening (Panel A) and percentage of lumen stenosis (B) of cuffed femoral arteries in ApoE3LeidenIL10^{-/-} and their IL10^{+/+} control littermates, 14 days after cuff placement (n=8 per group, *p<0.02). Panel C represents haematoxylin-phloxine-saffron (HPS) staining of cuffed femoral arteries of both groups. Neointimal surface (indicated by black line) is clearly increased in the IL10 knock-out group. Asterisks (*) indicate macrophage-derived foam cells (magnification 250x).

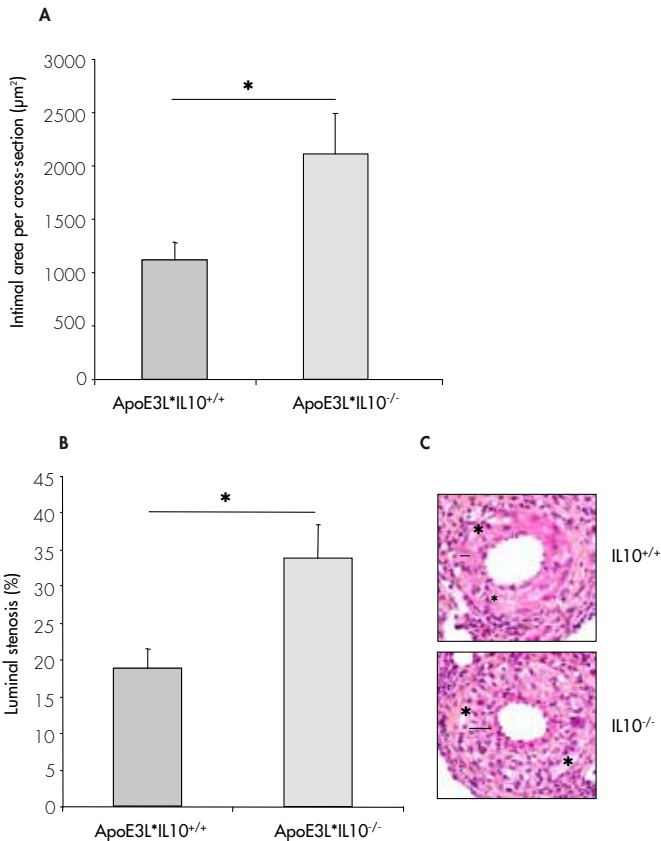


Figure 3.2: Expression of IL10 and Luciferase after intramuscular, non-viral gene therapy. Panel A: Murine IL 10 serum levels in ng/ml, one and three weeks after intramuscular electroporation of mIL10 cDNA or Luciferase as a control (n=5 per group, *p<0.01). IL10 protein levels are significantly increased as compared to the control group after electroporation at both time points. Panel B: Representative bioluminescence images of intramuscular luciferase expression at t=7 and 21 days after electrodelivery of Luciferase. Panel C: Quantitative reproduction of luciferase expression as measured with bioluminescence imaging (n=3).

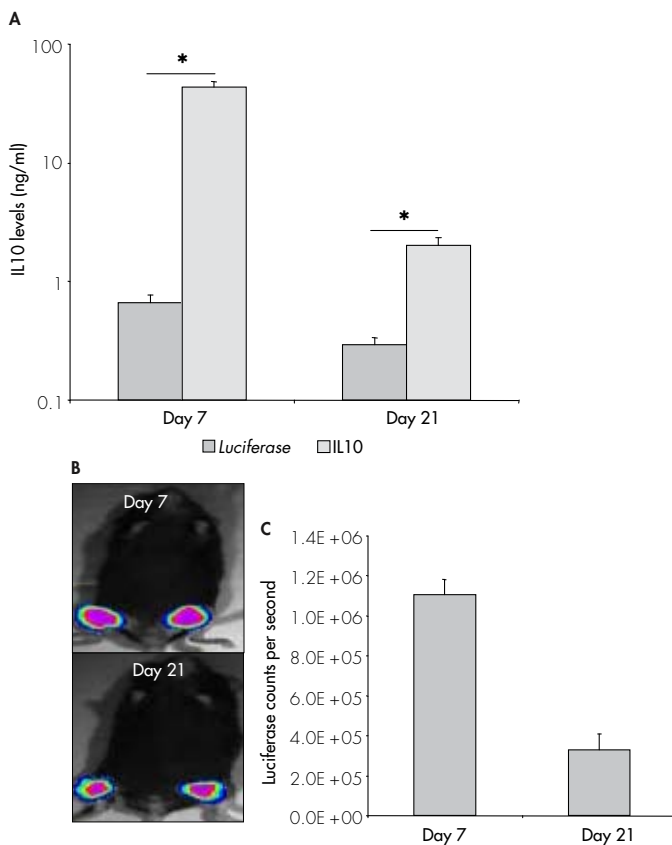


Figure 3.3: Effect of IL10 overexpression on neointima formation in hypercholesterolemic ApoE3Leiden mice. Total intimal area (Panel A) and percentage of lumen stenosis (B) of cuffed femoral arteries in hypercholesterolemic ApoE3Leiden mice, three weeks after electroporation of pCAGGS-mIL10 and pCAGGS-Luciferase as a control (n=8 per group, *p<0.02). Panel C represents haematoxylin-phloxine-saffron (HPS) staining of cuffed femoral arteries after electroporation. IL10 overexpression results in a marked reduction of neointima formation (intimal area is indicated by black line and asterisks (*) indicate macrophage-derived foam cells, magnification 200x).

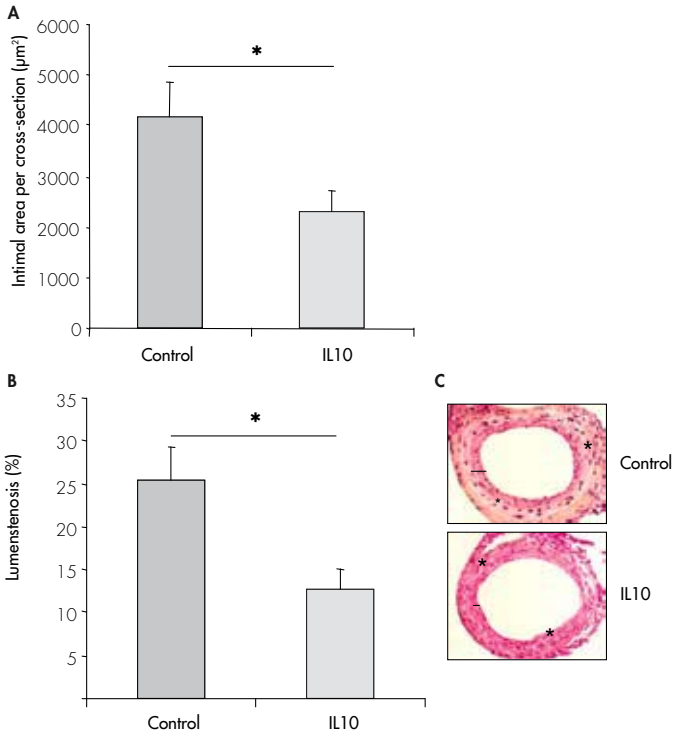
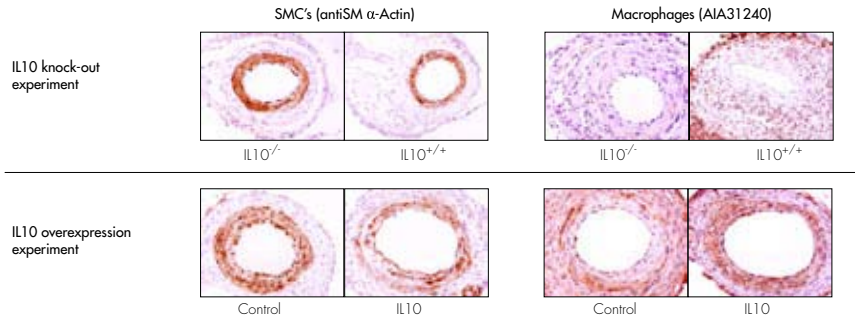
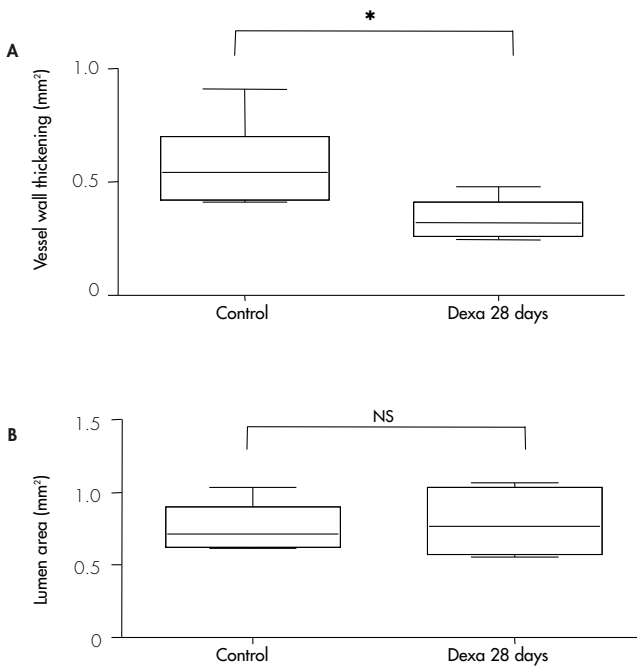


Figure 3.4: Effect of IL10 on relative SMC and macrophage content of medial and intimal areas. *Representative cross-sections of cuffed femoral arteries of both, IL10 knock-out and IL10 overexpression experiments, immunohistochemically stained for smooth muscle cells (antiSM α -Actin) and macrophages (AIA31240). Magnification 200x.*



LEGENDS CHAPTER 4

Figure 4.1: Dexamethasone treatment (0.15mg/kg/day in drinking water) reduces vein graft thickening in hypercholesterolemic ApoE3-Leiden mice after 28 days of treatment. Panel A: Quantification of vein graft thickening shows a reduction of 43% in the dexamethasone-treated animals, as compared to controls (n=6, * represents $P < .05$), whereas no significant changes in luminal area were observed (Panel B). Panel C: Representative cross-section, arrows indicate thickened vessel wall (HPS staining, magnification 40x). No differences are seen in the cellular composition of thickened grafts in both groups, as determined by computer-assisted morphometric analysis. Panel D: α -SM-actin staining representing vascular SMC. Panel E: AIA31240 staining representing macrophages.



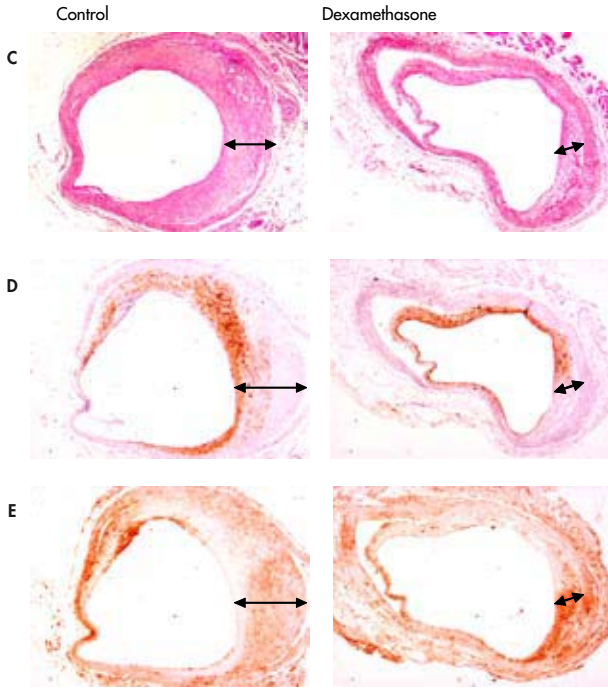
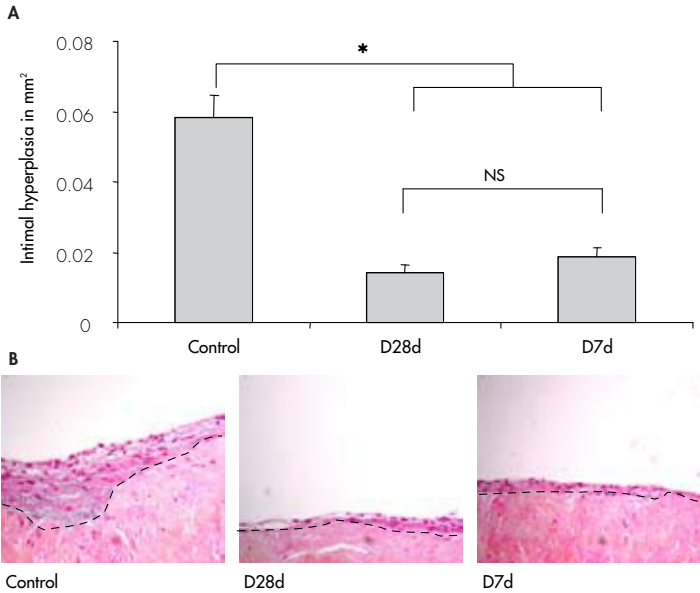
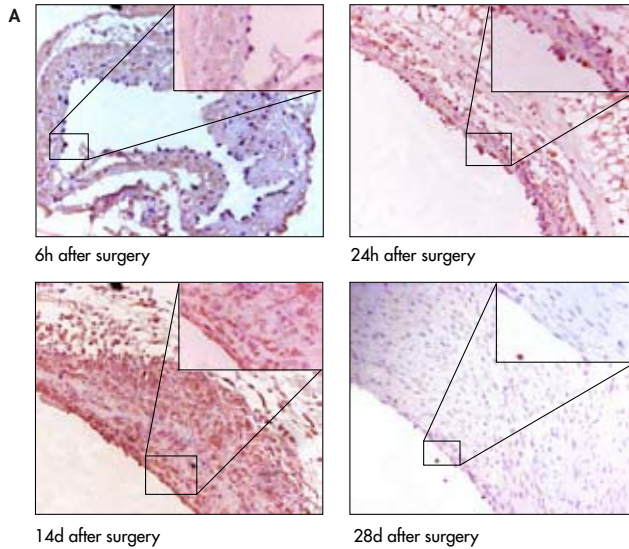


Figure 4.4: Effect of either short-term (D7d) or prolonged (D28d) dexamethasone exposure (0.75mg/ml medium) in IH formation in human saphenous vein organ cultures (n=12 per group). In both dexamethasone exposed groups a significantly lowered amount of IH was seen, when compared to the control segments (* represents $P < .05$, magnification 100x, dotted line indicates border separating media from intima).



LEGENDS CHAPTER 5

Figure 5.1: Panel A shows representative cross-sections of murine vein grafts harvested after several time points. MCP-1 expression in vein grafts identified by immunohistochemistry was seen mainly in endothelial cells, adhering monocytes and in the infiltrating cells of the developing IH. Inserts indicate adhering monocytes expressing MCP-1 (6h and 24h) and MCP-1 expression in the developing IH (14d).



Panel B represents the immunohistochemical detection of MCP-1 in cultured human saphenous veins. MCP-1 is abundantly present in the media at early time points and predominantly in IH at later time points after 14 and 28 days. Inserts indicate MCP-1 expressing endothelium and SMC (directly after excision and 24h) and MCP-1 expression in IH (28d). Magnification of all pictures 150-600x.

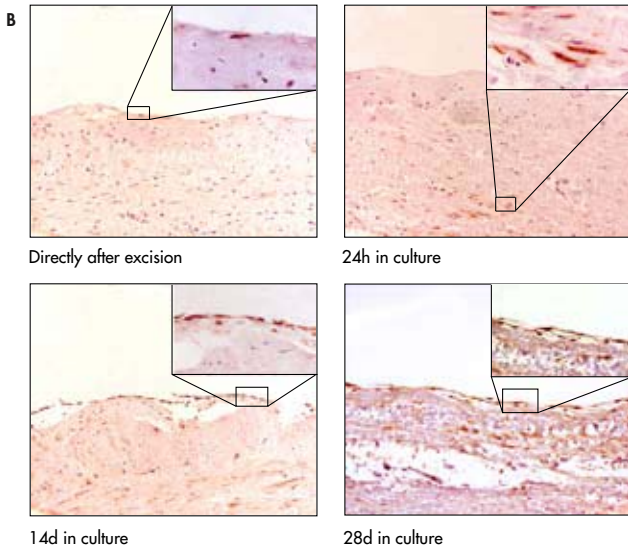


Figure 5.2: Effect of 7ND-MCP-1 gene-transfer on development of IH in murine vein grafts. Panel A: Significantly reduced IH surface is seen in the 7ND-MCP-1-treated group ($n=6$ per group, $p<0.05$). Panel B: Immunohistochemical staining for macrophages and smooth muscle cells. No differences in cellular composition of the lesions were observed (* represents $p<0.05$).

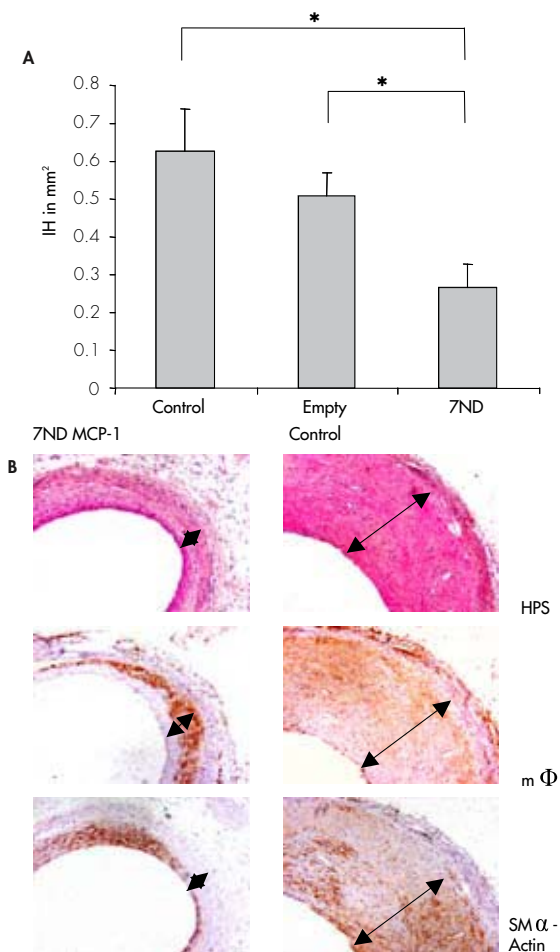
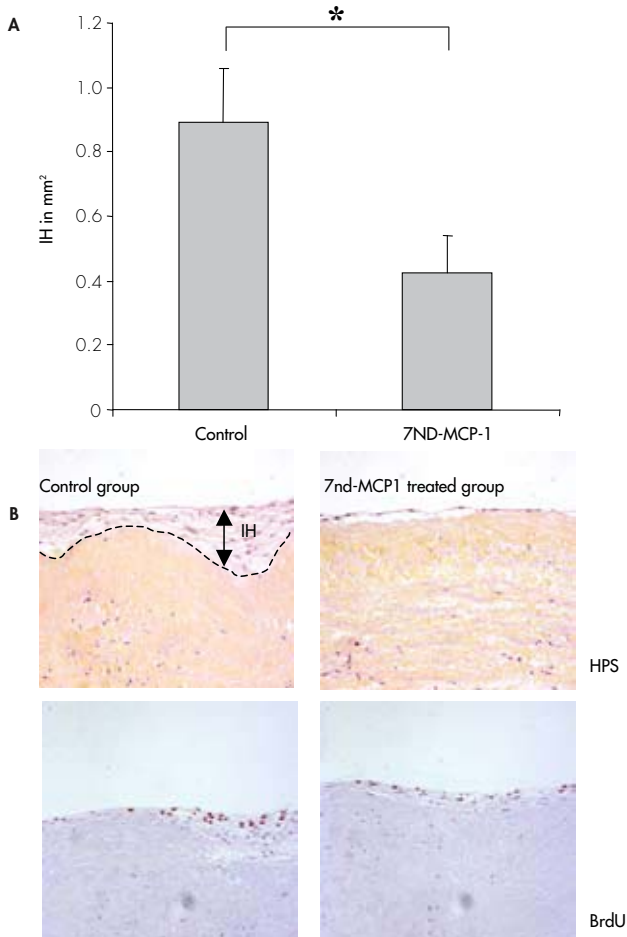


Figure 5.3: Effect of 7ND-MCP-1 on IH in HSV 28 days in culture. Panel A: Reduction in IH (n=12 per group) when exposed to conditioned medium containing 7ND-MCP-1 (* represents $p < 0.05$). Panel B: Representative cross section of HSV, strong reduction in both IH surface and BrdU-positive cells can be detected.



LEGENDS CHAPTER 6

Figure 6.1: Expression of MIP-1 α and RANTES in remodeling vein grafts as shown by immunohistochemistry. Panel A shows MIP-1 α - expression in the adhering leucocytes 1 day after engraftment, and presence of MIP-1 α in the thickened vessel wall at later time points. Panel B depicts RANTES presence in the vein graft wall at the early time-points. In the later stages of vein graft thickening diffuse distribution is seen in the intimal hyperplasia but predominantly in the adventitia of the vein grafts. (n=3 per time-point, magnification 125-300x, * represents lumen, arrow indicates vessel wall thickening).

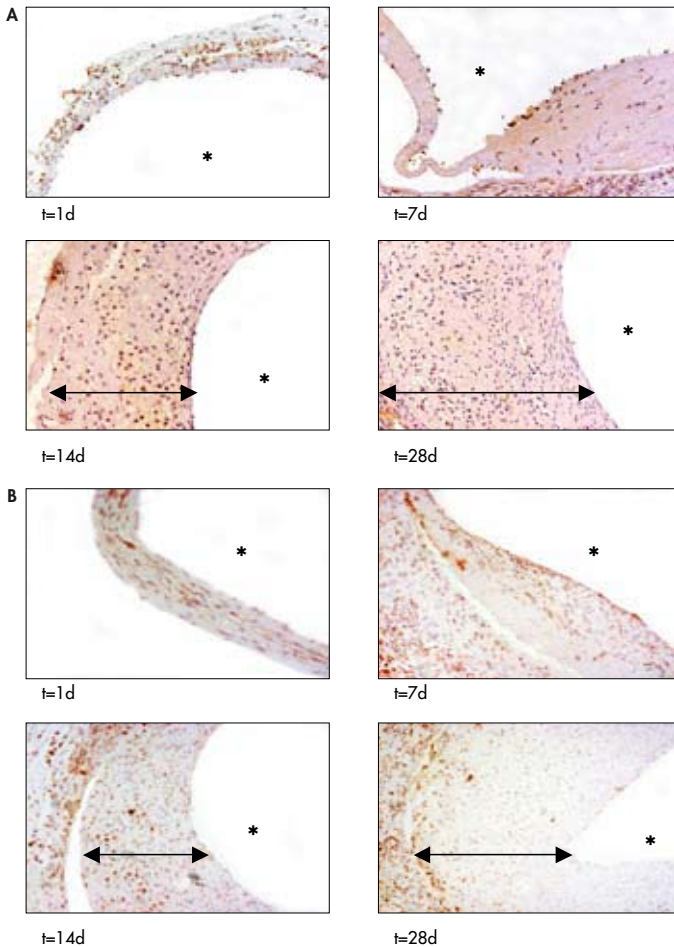
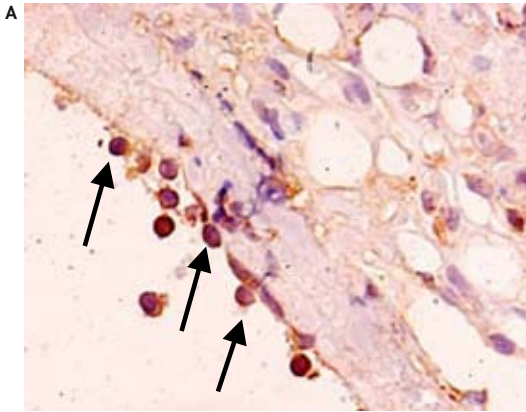


Figure 6.3: Panel A: Representative picture showing adhering AIA31240 positive cells (some are indicated by arrows; magnification 400x).



Panel B: Number of adhering AIA31240 positive cells (monocytes) 3 days after engraftment in Met-RANTES-treated and control vein grafts (analysis by immunohistochemistry, n=8 per group, at least 6 cross-sections per mice were analyzed). Data are expressed as mean±SEM.

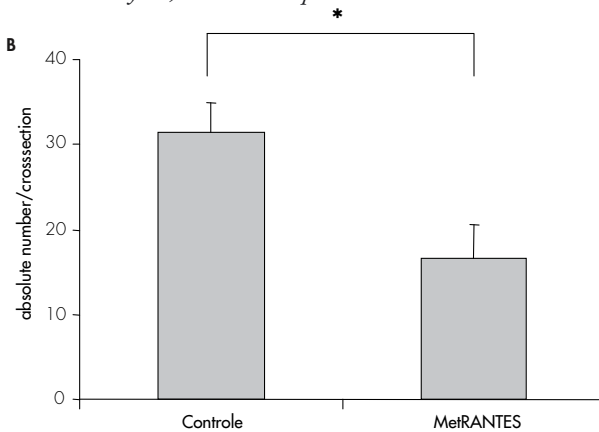
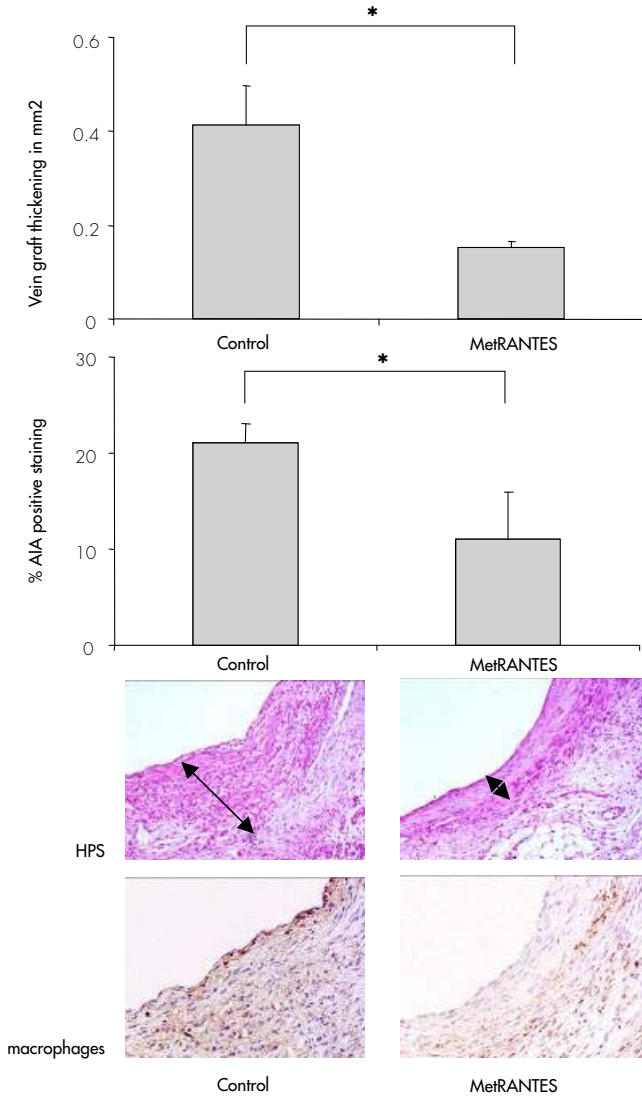


Figure 6.4: Effect of Met-RANTES on vein graft thickening and plaque composition (n=8 per group). Panel A displays the quantified data of both vein graft thickening and macrophage content of the plaque as defined by percentage of staining positive for AIA31240. Panel B shows representative pictures of HPS and AIA 31240 staining (magnification 200x, arrows indicate thickened vein graft wall).



LEGENDS CHAPTER 7

Figure 7.1: Expression of complement factors in thickened murine vein graft of ApoE3Leiden mice, 28 days after surgery. Massive intima hyperplasia formation vein graft thickening is observed, as indicated with arrows (HPS). The cellular composition (consisting of smooth muscle cells and macrophage-derived foam cells) of the thickened vein graft is shown. Immunohistochemical detection of complement factors C1q, C3 and C9. Both C1q and C3 are abundantly present in the deeper parts of the intimal hyperplasia co-localizing with foam cells. Furthermore, C1q and C3 are expressed in the endothelial layer and in inflammatory cells (mainly macrophages) adhering to the vessel wall and present in the adventitia. C9 is not detectable in the endothelium and inflammatory cells. However, like C1q and C3, it is present in the deeper parts of the intimal hyperplasia.

Regulatory enzymes CD59 and Crry in vein grafts demonstrate a different expression pattern. CD59 shows a diffuse expression throughout the thickened vein graft, whereas expression of the membrane-bound Crry shows a patchy, cell bound distribution, and is mainly localized in the media and adventitia of the murine vein graft. Magnification of all pictures 150x.

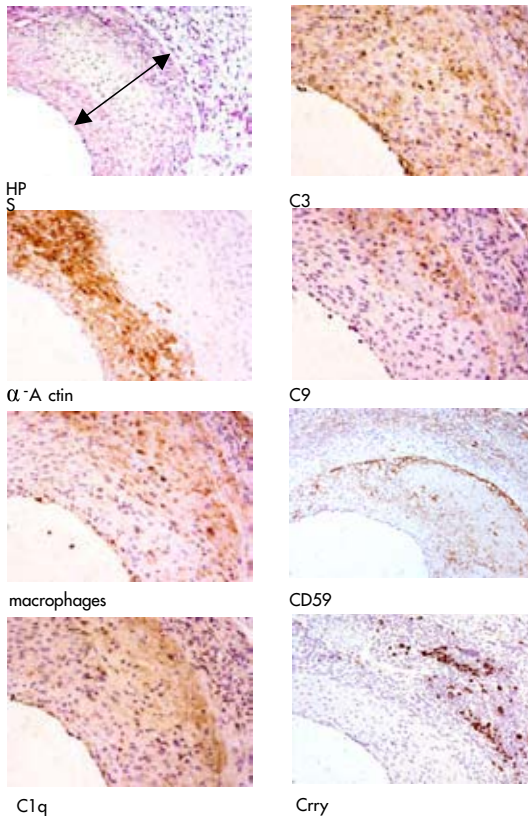
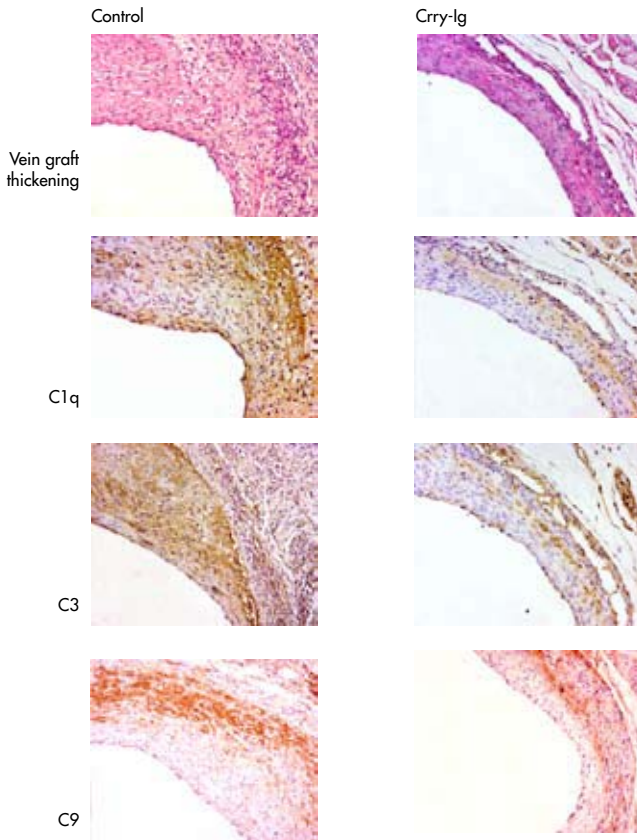


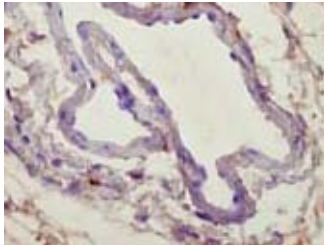
Figure 7.3: Effect of Crry-Ig treatment on development of intimal hyperplasia and accelerated atherosclerosis in murine vein grafts. Quantitative analysis of the effect of Crry-Ig treatment on development of intimal hyperplasia and accelerated atherosclerosis in murine vein grafts and C1q, C3 and C9 deposition in the vein grafts.



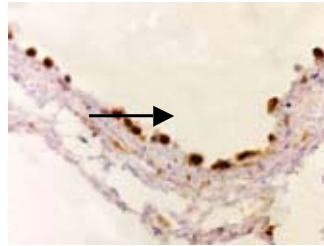
Representative cross section demonstrating reduced vein graft thickening, similar amounts of C1q deposition, and reduced C3 and C9 deposition (magnification 150x).

LEGENDS CHAPTER 8

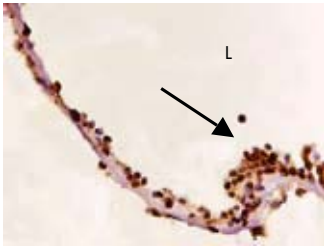
Figure 8.1: Detection of C5 in time in venous bypass grafts by immunohistochemistry. As soon as 6 hours after surgery, presence of C5 is seen in adhering leucocytes (appointed by arrows). Highest amounts of C5 are seen 3 to 7 days after surgery, and C5 remains present in later time-points predominantly in endothelial cells, foam cells and adventitial fibroblasts (magnification 150x (28d)-400x (6h)).



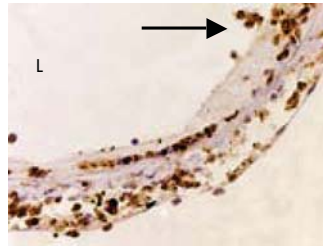
Normal caval vein



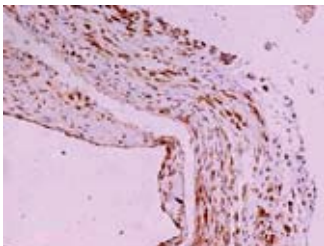
6h



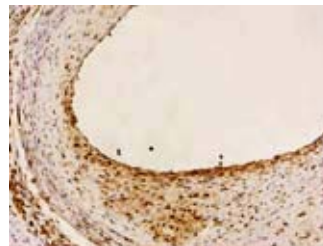
24h



3d



14d



28d

Figure 8.3: Effect of C5a recombinant protein application to vein grafts of hypercholesterolemic mice. Representative cross-sections of vein grafts exposed to either 20% PG and 20% PG containing 0.5 μ and 5 μ C5a recombinant protein (panel A, HPS staining). A dose-dependent increase in vein graft thickening was seen in the C5a-treated mice (panel B) (0.5 μ : $p=0.1$, 5 μ : $p=0.002$; arrows indicate vessel wall surface, magnification 200x).

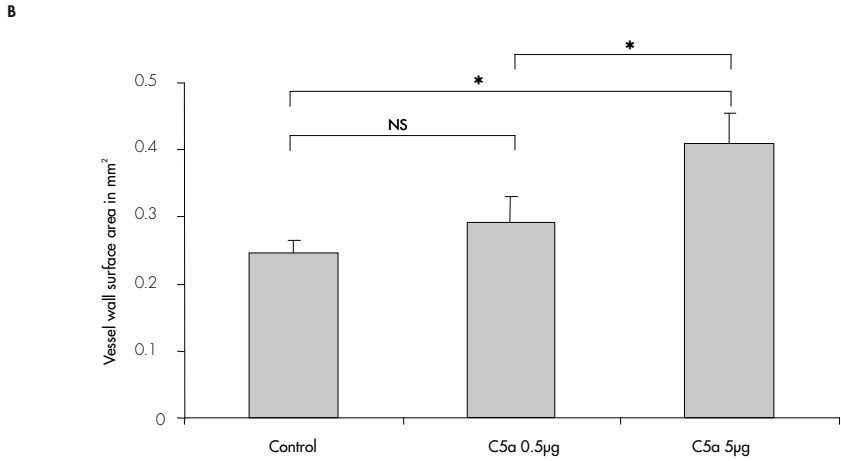
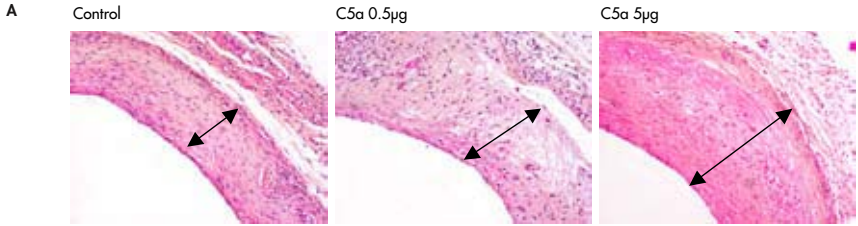


Figure 8.4: Effect of C5a application to vein grafts on foam cell contribution in lesion. Increased exposure to C5a results in a significant increase in foam cell contribution in the lesions (panel B). Panel A displays representative cross sections of immunohistochemistry using antibodies against macrophage derived foam cells, whereas arrows indicate positive staining against monocytes/foam cell (0.5µg: $p=0.1$, 5µg: $p<0.001$; magnification 200x).

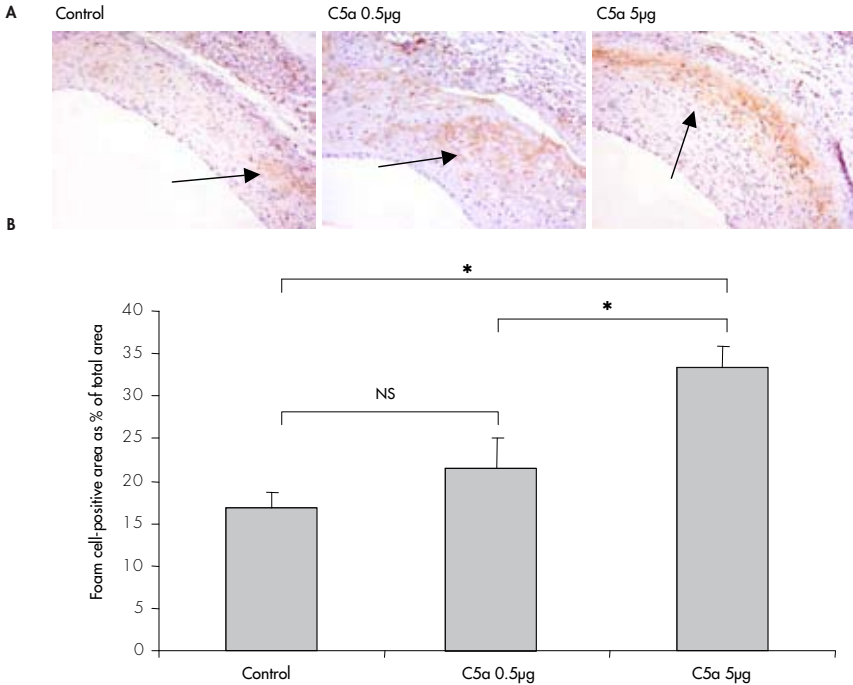
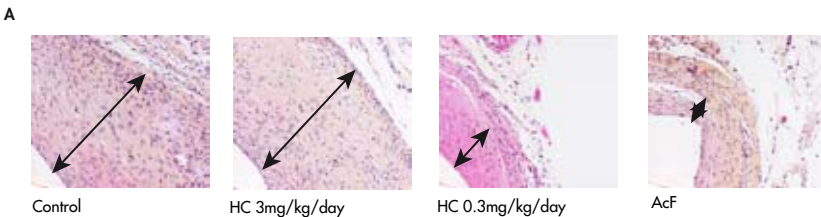
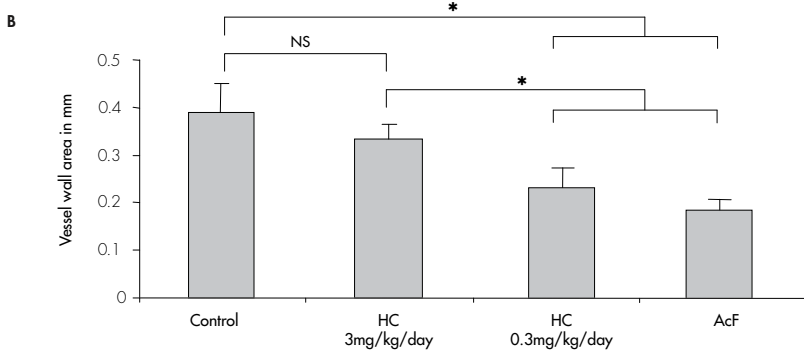


Figure 8.5: Effect of treatment with C5a receptor antagonists, HC and AcF. Panel A: Representative cross sections of control and treated vein grafts 28 days after surgery; a decrease in vein graft thickening is seen in the AcF and HC 0.3mg/kg/day treated groups (HPS staining, magnification 200x).



Panel B: Quantification of vessel wall surface in mm² control and treated vein grafts 28 days after surgery (n=7 per group, *represents p<0.05); C5aRA treatment results in decrease in vein graft thickening 28 days after surgery.



Panel C: Quantification of macrophages-derived foam cells contribution in the vessel wall by immunohistochemistry, described as percentage of total vessel wall surface; treatment with C5aRA results in a decrease in foam cell content in the vessel wall (n=7 per group, *represents p<0.05).

